Sliding Mode Control of Biglide Planar Parallel Manipulator

Mustapha Litim[1], Benyamine Allouche[2], Abdelhafid Omari[1], Antoine Dequidt[2]
and Laurent Vermeiren[2]

[1]*Department of Automatic USTO\LDDE, USTO-MB University, USTO, Oran, Algeria*

[2]*UVHC LAMIH CNRS, UMR 8201, University of Valenciennes and Hainaut-Cambresis, Valenciennes, France*

Abstract: This work presents the control of a two-degree of freedom parallel manipulator using nonlinear sliding mode approach. The aim is to achieve a robust control for trajectory tracking. The control is based on the inverse dynamic model in the Cartesian space of the parallel manipulator. Kinematic analysis are also discussed. To guarantee the high performance on the tracking control. Biglide robot requires full knowledge on the system's dynamics. In this paper, some important properties of the parallel manipulators are considered to develop a sliding mode controller which can drive the movement tracking error to zero asymptotically. Numerical simulations are completed to show the effectiveness of the approach for a large parameter variations.

1 INTRODUCTION

Parallel Robots are closed loop kinematic chain mechanisms. They have several advantages compared to serial link manipulator, such as high accuracy, high stiffness, high payload capability and low moving inertia, etc. Therefore, they attracted a lots of researchers's interests in recent decades (Omran, A and Elshabasy, M. 2010) (Cheng, H., Yiu, Y. K., and Li, Z., 2003). They are widely used in different applications, such as machine tools (Abdellatif, H., Grotjahn, M., and Heimann, B. 2005), industrial high speed applications (Weck, M., Staimer, D. 2002), medical robots, micro robots (Jamwal, P. K., Xie, S. Q., Tsoi, Y. H., and Aw, K. C. 2010), humanoid robots and flight simulators by (Gough, V. E. 1956) (Stewart, D. 1965). Despite of their advantages, parallel robots have also some drawbacks, such as limited workspace and complex kinematic issues caused by the presence of multiple closed loop chains and singularities. In this paper, we will discuss the motion control of a planar parallel robot with two degrees of freedom (DOF) (Vermeiren, L., Dequidt, A., Afroun, M., and Guerra, T. M. 2012).

(Cheung, J. W., Hung, Y. S. 2005),(Pierrot, F., Krut, S., Baradat, C., and Nabat, V. 2011) are used These types of robots in the manufacturing industry of electronic products, as pick and place applications.

A dynamical analysis of parallel robot is very complex because the existence of multiple close-loop chains. In addition, due to uncertainties such as not modeled errors on dynamic parameters, measurement noise and external disturbances. Many researchers worked on the dynamic modeling of parallel robots as in (Khalil, W., Ibrahim, O. 2007), (Staicu, S., Liu, X. J., and Wang, J. 2007) and (Staicu, S. 2009).

The Conventional control methods of parallel manipulators have attracted many researchers in studying their performances. A proportional derivative (PD) controller (Ghorbel, F. H., Chtelat, O., Gunawardana, R., and Longchamp, R. 2000), a nonlinear PD controller (Ouyang, P. R., Zhang, W. J., and Wu, F. X. 2002) and an adaptive switching learning PD control method (Ouyang, P. R., Zhang, W. J., and Gupta, M. M. 2006), (Le, T. D., Kang, H. J., and Suh, Y. S. 2013) were proposed for the motion control of parallel manipulators. It is also noted in (Piltan, F., Rahmdel, S., Mehrara, S., and Bayat, R. 2012) that all of these controllers are simple and easy to implement but they are not robust in presence of uncertainties or when the robot supports different payloads. Some other advanced controllers were proposed, such as the computed torque controller (Vermeiren, L., Dequidt, A., Afroun, M., and Guerra, T. M. 2012), (Yang, Z., Wu, J., and Mei, J. 2007), and the adaptive controller (Zhu, X., Tao, G., Yao, B., and Cao, J. 2009). These approaches are based on a full knowledge dynamic model and require a computational power. However,

it is complicated to obtain a precise dynamic model of the parallel manipulators, due to the aforementioned drawback (Le, T. D., Kang, H. J., and Suh, Y. S. 2013).

In this paper, a new contribution is proposed to control parallel robot in the cartesian space . This approach is based on the inverse dynamic model and sliding mode technics (Vermeiren, L., Dequidt, A., Afroun, M., and Guerra, T. M. 2012). The theory of sliding mode control has been successfully applied to serial manipulators (Slotine, J. J. E., Li, W. 1991), (Sadati, N., Ghadami, R. 2008) and (Zeinali, M., Notash, L. 2010). This approach exhibits the property of robustness for its ability to reject the uncertainties and the external disturbances which satisfy the matching conditions (Castaos, F., Fridman, L. 2006), (AL-Samarraie, S. A. 2013). The advantage of sliding mode is low sensitivity versus parameter variations and disturbances. The design of sliding mode controller consists in two steps: The choice of the sliding variable according to the control objective. While the second is to use a discontinuous control to force the state trajectories of the system to reach the sliding surface in a finite time and to evolve on it in spite of disturbance.(AL-Samarraie, S. A. 2013), (Utkin, V., Guldner, J., and Shijun, M. 1999). Sliding mode control has been used for several applications such as Underwater vehicles (Sankaranarayanan, V., Mahindrakar, A. D. 2009), Active vehicle suspensions (Geravand, M., Aghakhani, N. 2010), Magnetic levitation (Lin, F. J., Chen, S. Y., and Shyu, K. K. 2009), DC-DC converters (Tan, S. C., Lai, Y. M., and Tse, C. K. 2008) and photovoltaic solar in (Khiari, B., Sellami, A., Andoulsi, R., and Mami, A. 2012).

This paper is organized as follows. In Section2, the dynamic model of 2-DOF parallel manipulator is formulated in the Cartesian space. In Section3, sliding mode controller is developed and applied to the inverse dynamic model of robot in Cartesian space the Section4, presents simulation results of the proposed controller. Finally, some conclusions are presented in the closing section.

2 DYNAMICS MODELING OF BIGLIDE PARALLEL ROBOT

2.1 Kinematic and Geometric Analysis

For the geometric and kinematics modeling of a Biglide parallel manipulator, the following conventions are used according to (Vermeiren, L., Dequidt, A., Afroun, M., and Guerra, T. M. 2012). The manip-

ulator provides 2DOF of translation on the XY plane, the positioning of end effector is represented by operational variables (x, y) driven by two prismatic active joints (q_1, q_2) in the same X axis.

The operational vector is then written as follow:

$$P = [x \quad y]^T \tag{1}$$

The generalized joint variable vector is:

$$q = [q_1 \quad q_2]^T \tag{2}$$

The mechanism has two constant length struts with moveable foot points Figure 1. Both struts have the same lengtha. The relationship between both coordinate vectors is written with kinematic loop-closure constraints Figure 1:

$$\Phi(P,q) = 0, \Phi(P,q) = \begin{pmatrix} (x - q_1)^2 + y^2 - a^2 \\ (q_2 - x)^2 + y^2 - a^2 \end{pmatrix}. \tag{3}$$

The Inverse geometric model (IGM) formula is given by:

$$q = g(P) \tag{4}$$

with

$$g(P) \equiv \begin{pmatrix} x - C(y) \\ x + C(y) \end{pmatrix}, C(y) \equiv \sqrt{a^2 - y^2} \tag{5}$$

The direct geometric model (DGM) can be derived from (4):

$$P = g^{-1}(q) \tag{6}$$

with

$$g^{-1}(q) = \begin{pmatrix} \frac{q_1 + q_2}{2} \\ \sqrt{a^2 - \frac{(q_1 + q_2)^2}{4}} \end{pmatrix} \tag{7}$$
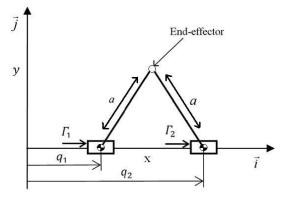

Figure 1: kinematic schemes of Biglide robot.

The relation between the joint space and the operational space is conveniently described by two

Jacobian matrices $J_p(P,q)$ and $J_q(P,q)$ is given as:

$$J_p(P,q)\dot{P} = J_q(P,q)\dot{q} \qquad (8)$$

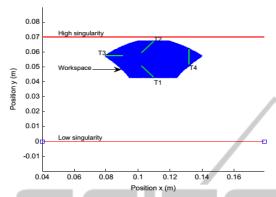The parallel singularities occur when the Jacobian

Figure 2: Workspace and trajectories: ($T1$) Low trajectory, ($T2$) High trajectory, ($T3$) Left trajectory, and ($T4$) Right trajectory.

matrix J_p is rank deficient. The Biglide has two parallel singularities: (Vermeiren, L., Dequidt, A., Afroun, M., and Guerra, T. M. 2012)

• High singularity: $q_1 = q_2 = x$, the struts are superposed and $y = 0.07$, Figure 2.

• Low singularity: $y = 0$, the struts are aligned, Figure 2

The kinematic relationship between end-effector velocities and joint velocities is computed by differentiating (3) with respect to time:

$$J_p(P,q)\dot{P} = J_q(P,q)\dot{q} \ \text{ with } J_p(P,q) = \begin{bmatrix} x - q_1 & y \\ x - q_2 & y \end{bmatrix}$$

$$J_p(P,q) = \begin{bmatrix} x - q_1 & 0 \\ 0 & x - q_2 \end{bmatrix} \qquad (9)$$

2.2 Dynamic Model

The dynamics equations of the Biglide in operational space are given as follows (Vermeiren, L., Dequidt, A., Afroun, M., and Guerra, T. M. 2012):

$$\Gamma = M(P)\ddot{P} + N(P,\dot{P}) \qquad (10)$$

with

$P = \begin{bmatrix} x & y \end{bmatrix}^T$, $M(P)$ is the inertial matrix given as follow:

$$M(P) = \begin{pmatrix} m_1 + \frac{1}{2}(m - \lambda_1 + \lambda_2) & f_1(P) \\ m_2 + \frac{1}{2}(m - \lambda_2 + \lambda_1) & f_2(P) \end{pmatrix} \qquad (11)$$

with

$$\lambda_{1,2} = ms_{1,2}/a$$

$$f_1(P) = [(2m_1 - 3\lambda_1 - \lambda_2)y^2 + mC(y)^2 + J_1 \\ + J_2]/(2C(y) \times y)$$

$$f_2(P) = -[(2m_2 - 3\lambda_2 - \lambda_1)y^2 + mC(y)^2 + J_1 \\ + J_2]/(2C(y) \times y)$$

$$N(P,\dot{P}) = N(y,\dot{y}) + p(y)$$

$N(y,\dot{y})$ is a coriolis / centripetal matrix can be written as:

$$R(y,\dot{y}) = \begin{bmatrix} r_{11} & r_{12} \\ r_{21} & r_{22} \end{bmatrix} \qquad (12)$$

$$\begin{cases} r_{11} = r_{12} = 0 \\ r_{12} = -[(2m_1 - 3\lambda_1 - \lambda_2)y^2 + (2m_1 - 3\lambda_1 - \lambda_2) \\ C(y)^2 + J_1 + J_2]\dot{y}/(2C(y)^3 \\ r_{22} = [(2m_2 - 3\lambda_2 - \lambda_1)y^2 + (2m_2 - 3\lambda_2 - \lambda_1) \\ C(y)^2 + J_1 + J_2]\dot{y}/(2C(y)^3 \end{cases}$$

$p(y)$ is a vector containing gravity torques can be written as:

$$p(y) = \begin{pmatrix} (gC(y)(m + \lambda_1 + \lambda_2))/2y \\ (-gC(y)(m + \lambda_1 + \lambda_2))/2y \end{pmatrix} \qquad (13)$$

3 CONTROLLER DESIGN

In this section the control law based on sliding mode approach is applied on the inverse dynamic model in operational space of the Biglide.

From equation (10), the direct dynamic model in operational space is given as fallow:

$$\ddot{P} = M(P)^{-1}[\Gamma - N(P,\dot{P})] \qquad (14)$$

with

$P = \begin{bmatrix} x & y \end{bmatrix}^T$ is x and y vector positions of the end-effector.

$\Gamma = \begin{bmatrix} \Gamma_1 & \Gamma_2 \end{bmatrix}^T$ is torque vector.

3.1 Sliding Mode Control

The tracking control problem in operational space is to find a control law such that given a desired trajectory P_{des}, and the tracking error e_i is go to zero asymptotically.

where

$$e_i = P_{mes} - P_{des}, i = (1,2). \qquad (15)$$

with

$P_{mes} = \begin{bmatrix} x_{mes} & y_{mes} \end{bmatrix}^T$ is measure position vector of the end-effector.

$P_{des} = \begin{bmatrix} x_{des} & y_{des} \end{bmatrix}^T$ is desired position vector of the end-effector.

The relative degree of the system from (8) $r = 2$, the sliding surface selected in our work is given by:

$$S = \dot{e} + \lambda e \qquad (16)$$

where λ is $2 * 2$ diagonal positive definite matrix.

Consider the following Lyapunov function candidate

$$V = \frac{1}{2} S^T S \qquad (17)$$

Time derivative of (11) will lead to

$$\dot{V} = S^T \dot{S} \qquad (18)$$

In which the term $\dot{S}$ is given by

$$\dot{S} = \lambda \dot{e} + \ddot{P}_{mes} - \ddot{P}_{des} \qquad (19)$$

where

$$\ddot{P}_{mes} = M(P)^{-1}[\Gamma - N(P,\dot{P})] \qquad (20)$$

with
$\ddot{P}_{mes} = \begin{bmatrix} \ddot{x}_{mes} & \ddot{y}_{mes} \end{bmatrix}^T$ is measure acceleration vector of the end-effector.

Taking (20) for $\ddot{P}_m$ and substituting in (19) results in

$$\dot{S} = \lambda \dot{e} - \ddot{P}_{des} + M(P)^{-1}[\Gamma - N(P,\dot{P})] \qquad (21)$$

From equation (20) we can write equation (18) as

$$\dot{V} = S^T[\lambda \dot{e} - \ddot{P}_{des} + M(P)^{-1}[\Gamma - N(P,\dot{P})]] \qquad (22)$$

From Lyapunov stability theory we know that the system reaches $S = 0$ in finite time of the above Lyapunov function and $\dot{V} = S\dot{S} < 0$
Defining the control signal as

$$\Gamma = \hat{\Gamma} - MK sgn(S) \qquad (23)$$

with

$\Gamma = \begin{bmatrix} \Gamma_1 & \Gamma_2 \end{bmatrix}^T$

and $\hat{\Gamma}$ is defined as

$$\hat{\Gamma} = [M(P)(P_{des} - \lambda \dot{e}) + N(P,\dot{P})] \qquad (24)$$

will cause

$$\dot{S} = -K sign(S) \qquad (25)$$

with
$K \in R^{2*1}$ is the gain and $sign(S)$ is switching function.

Hence, according to the Lyapunov theory the control law (22) will result in a stable closed loop system. In practice, the control law (22) cannot be used because of containing the term $sign(S)$ which results in high frequency oscillations, called chattering, and it is replaced by a continuous approximation. Chattering may be reduced by using a high saturation function. We define control law and tracking as

$$\Gamma = \hat{\Gamma} - MK sat(S) \qquad (26)$$

where $sat(S)$ is a saturation function and can be defined as follow

$$sat(S(t)) = \begin{cases} \dfrac{S(t)}{\|S(t)\|} & si \quad S(t) \geq \delta \\ \dfrac{S(t)}{\|S(t) + \delta\|} & si \quad S(t) < \delta \end{cases}$$

which provide a very smooth control action.

4 SIMULATION RESULTS

The Biglide manipulator is tested in simulation in order to validate sliding mode controller. The reference trajectory tracking (a 5th order polynomial interpolation), The numerical parameters simulation of dynamic model are defined from Table I in Appendix.

- CTC: Computed Torque Control (Vermeiren, L., Dequidt, A., Afroun, M., and Guerra, T. M. 2012);
- SMC: sliding mode Control, Eqs. (22);

The model of the parallel robot used for numerical simulation includes structured and unstructured uncertainties. The structured uncertainty is considered for a variation of the end effector mass corresponding to $\Delta m = 0.816 kg$ of course no uncertainty corresponds to $\Delta m = 0$.
Simulation has been performed in-order to examine the effectiveness of proposed controller design.

4.1 Discussion of Simulation Results

The simulation results of CTC controller (Vermeiren, L., Dequidt, A., Afroun, M., and Guerra, T. M. 2012) and sliding mode controller are presented in Figs. 2 and 4 for the trajectories $T1$ (near to workspace low boundary) and Figs. 3 and 5 for $T2$ (near to workspace high boundary), for each figure trajectories, parts (a) and (b) present the set Point and the response along x and y axes and parts (c) and (d) present the control input of both actuators.
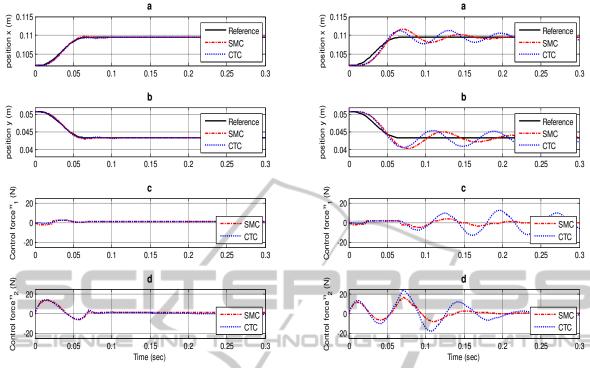
Figure 3: Control schemes for low trajectory (T1) and $\Delta m = 0$.

Figure 5: Control schemes for low trajectory (T1) and $\Delta m = 0.816$.
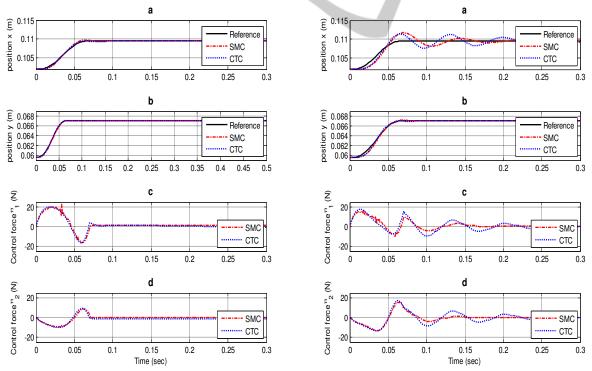
Figure 4: Control schemes for high trajectory (T2) and $\Delta m = 0$.

Figure 6: Control schemes for high trajectory (T2) and $\Delta m = 0.816$.

307

Note also that Figs. 2 and 3 are without mass variation $\Delta m = 0$ Where as Figs. 4 and 5 uses a $\Delta m = 0.816 Kg$. The mass variation is used to check the robustness of these controllers. In the former case, $\Delta m = 0$, going from the best to the worst; The sliding mode Controller and CTC controller shows a good capability of response. Based on Figure 4 and 5; by comparing response trajectory with mass variation of platform $, \Delta m = 0.816 Kg$ the sliding mode control presents the good results according to structured uncertainties (parametric variation), and for the CTC which is presents some important overshoot with some oscillation in trajectory response. In order to quantify the behavior of the controllers CTC and sliding mode controller some well-known criteria are computed for 4 trajectories $T1, T2, T3$ and $T4$ in the work space (Vermeiren, L., Dequidt, A., Afroun, M., and Guerra, T. M. 2012). The criteria is computed over a time simulation of $T = 2_s$ using the error vector, and the control force input vector.
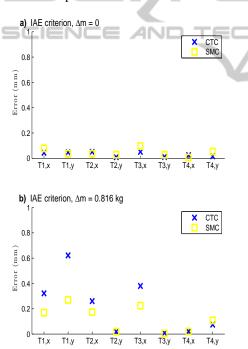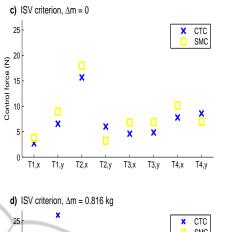
a) IAE criterion, $\Delta m = 0$

b) IAE criterion, $\Delta m = 0.816$ kg

Figure 7: (a)-(c) Performance criteria (position error and control force) computed for all displacements ($T1$&$T4$) trajectories along x and y axes), $\Delta m = 0$.

From the Fig. 6 and 7 for all trajectories the sliding mode control shows a good tracking performance for all displacement ($T1, T2, T3, and T4$). The results confirm previous observations. with mass variations, the sliding mode is more robust and sensitive to each parametric change compared with CTC controller.
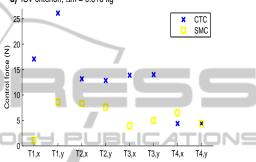
c) ISV criterion, $\Delta m = 0$

d) ISV criterion, $\Delta m = 0.816$ kg

Figure 8: (b)-(d) Performance criteria (position error and control force) computed for all displacements ($T1$&$T4$) trajectories along x and y axes), $\Delta m = 0.816$.

5 CONCLUSION

This paper, present different results of a nonlinear control approach applied to a planar $2DOF$ parallel manipulator Biglide type. Using sliding mode control approach to achieve a best performance and robust control for trajectory tracking, the control is based on the inverse dynamic model in the Cartesian space of the parallel manipulator. The sliding mode is employed successfully for the regulation and tracking of a multi input multi output planer parallel robot in presence of nonlinearities. Stability analysis based on Lyapunov theory is performed to guarantee global, asymptotic and exponential convergence.

REFERENCES

Omran, A and Elshabasy, M. (2010). A note on the inverse dynamic control of parallel manipulators. In *Proceedings of the Institution of Mechanical Engineers, Part C: Journal of Mechanical Engineering Science, 224(1), 25-32.*

Cheng, H., Yiu, Y. K., and Li, Z. (2003). Dynamics and control of redundantly actuated parallel manipulators. Mechatronics. *IEEE/ASME Transactions on, 8(4), 483-491.*

Abdellatif, H., Grotjahn, M., and Heimann, B. (2005, December). High efficient dynamics calculation approach for computed-force control of robots with parallel structures. *In Decision and Control, 2005 and 2005 European Control Conference. CDC-ECC'05. 44th IEEE Conference on (pp. 2024-2029). IEEE.*

Weck, M., Staimer, D. (2002). Parallel kinematic machine toolscurrent state and future potentials. *CIRP Annals-Manufacturing Technology, 51(2), 671-683.*

Jamwal, P. K., Xie, S. Q., Tsoi, Y. H., and Aw, K. C. (2010). Forward kinematics modelling of a parallel ankle rehabilitation robot using modified fuzzy inference. *Mechanism and Machine Theory, 45(11), 1537-1554.*

Gough, V. E. (1956) Contribution to discussion of papers on research in automobile stability, control and tyre performance. *In Proc. Auto Div. Inst. Mech. Eng (Vol. 171, pp. 392-394).*

Stewart, D. (1965). A platform with six degrees of freedom. *Proceedings of the institution of mechanical engineers, 180(1), 371-386.*

Vermeiren, L., Dequidt, A., Afroun, M., and Guerra, T. M. (2012). Motion control of planar parallel robot using the fuzzy descriptor system approach. *ISA transactions, 51(5), 596-608.*

Cheung, J. W., Hung, Y. S. (2005, July) Modelling and control of a 2-DOF planar parallel manipulator for semiconductor packaging systems. *In Advanced Intelligent Mechatronics. Proceedings, 2005 IEEE/ASME International Conference on (pp. 717-722). IEEE.*

Pierrot, F., Krut, S., Baradat, C., and Nabat, V. (2011). Par2: a spatial mechanism for fast planar two-degree-of-freedom pick-and-place applications. *Meccanica, 46(1), 239-248.*

Khalil, W., Ibrahim, O. (2007). General solution for the dynamic modeling of parallel robots. *Journal of intelligent and robotic systems, 49(1), 19-37.*

Staicu, S., Liu, X. J., and Wang, J. (2007). Inverse dynamics of the HALF parallel manipulator with revolute actuators. *Nonlinear Dynamics, 50(1-2), 1-12.*

Staicu, S. (2009). Recursive modelling in dynamics of Agile Wrist spherical parallel robot. *Robotics and Computer-Integrated Manufacturing, 25(2), 409-416.*

Ghorbel, F. H., Chtelat, O., Gunawardana, R., and Longchamp, R. (2000). Modeling and set point control of closed-chain mechanisms: theory and experiment. *Control Systems Technology, IEEE Transactions on, 8(5), 801-815.*

Ouyang, P. R., Zhang, W. J., and Wu, F. X. (2002). Nonlinear PD control for trajectory tracking with consideration of the design for control methodology. *In Robotics and Automation, 2002. Proceedings. ICRA'02. IEEE International Conference on (Vol. 4, pp. 4126-4131). IEEE.*

Ouyang, P. R., Zhang, W. J., and Gupta, M. M. (2006). An adaptive switching learning control method for trajectory tracking of robot manipulators. *Mechatronics, 16(1), 51-61.*

Le, T. D., Kang, H. J., and Suh, Y. S. (2013). Chattering-Free Neuro-Sliding Mode Control of 2-DOF Planar Parallel Manipulators. *Internation Journal of Advanced Robotic Systems (October 22, 2013).*

Piltan, F., Rahmdel, S., Mehrara, S., and Bayat, R. (2012). Sliding mode methodology vs. Computed torque methodology using matlab/simulink and their integration into graduate nonlinear control courses. *International Journal of Engineering, 6(3), 142-177.*

Yang, Z., Wu, J., and Mei, J. (2007). Motor-mechanism dynamic model based neural network optimized computed torque control of a high speed parallel manipulator. *Mechatronics, 17(7), 381-390.*

Zhu, X., Tao, G., Yao, B., and Cao, J. (2009) Integrated direct/indirect adaptive robust posture trajectory tracking control of a parallel manipulator driven by pneumatic muscles. *Control Systems Technology, IEEE Transactions on, 17(3), 576-588.*

Slotine, J. J. E., Li, W. (1991). Englewood Cliffs, NJ: Prentice-Hall. *Applied nonlinear control (Vol. 199, No. 1).*

Sadati, N., Ghadami, R. (2008). Adaptive multi-model sliding mode control of robotic manipulators using soft computing. *Neurocomputing, 71(13), 2702-2710.*

Zeinali, M., Notash, L. (2010). Adaptive sliding mode control with uncertainty estimator for robot manipulators. *Mechanism and Machine Theory, 45(1), 80-90.*

Castaos, F., Fridman, L. (2006). Analysis and design of integral sliding manifolds for systems with unmatched perturbations. *Automatic Control, IEEE Transactions on, 51(5), 853-858.*

AL-Samarraie, S. A. (2013). Invariant Sets in Sliding Mode Control Theory with Application to Servo Actuator System with Friction. *WSEAS TRANSACTIONS on SYSTEMS and CONTROL, 8(2), 33-45.*

Utkin, V., Guldner, J., and Shijun, M. (1999). Sliding mode control in electro-mechanical systems (Vol. 34). *CRC press.*

Sankaranarayanan, V., Mahindrakar, A. D. (2009). Control of a class of underactuated mechanical systems using sliding modes. *Robotics, IEEE Transactions on, 25(2), 459-467.*

Geravand, M., Aghakhani, N. (2010). Fuzzy sliding mode control for applying to active vehicle suspentions. *Wseas Transactions on Systems and Control, 5(1), 48-57.*

Lin, F. J., Chen, S. Y., and Shyu, K. K. (2009). Robust dynamic sliding-mode control using adaptive RENN for magnetic levitation system. *Neural Networks, IEEE Transactions on, 20(6), 938-951.*

Lin, F. J., Chen, S. Y., and Shyu, K. K. (2009). General design issues of sliding-mode controllers in DCDC converters. *Industrial Electronics, IEEE Transactions on, 55(3), 1160-1174*

Khiari, B., Sellami, A., Andoulsi, R., and Mami, A. (2012). A Novel Strategy Control of Photovoltaic Solar Pumping System Based on Sliding Mode Control. *International Review of Automatic Control, 5(2)*

APPENDIX

Numerical simulations include a model with structured and unstructured uncertainties based on the nominal model used to design the controller. Unmodeled dynamics such as elastic joints (Vermeiren, L., Dequidt, A., Afroun, M., and Guerra, T. M. 2012) between actuators and linkages and Stribeck friction (Vermeiren, L., Dequidt, A., Afroun, M., and Guerra, T. M. 2012) applied on prismatic joints appear in this augmented model to provide more realistic simulations.

The dynamics of the actuator writes:

$$\Gamma = M_a \ddot{q}_a + b\dot{q}_a + \Gamma_t + \Gamma_f \qquad (27)$$

with $q_a = [q_{a1} q_{a2}]^T$, $M_a = diag(m_a m_a)Z$, $\Gamma_f = [\Gamma_{f1} \Gamma_{f2}]^T Z$, the elastic joint model:

$$\Gamma_t = k_t(q_a - q) + b_t(\dot{q}_a - \dot{q}) \qquad (28)$$

and the Stribeck friction model of the dry friction:

$$\Gamma_{fi} = \begin{cases} [\Gamma_{fc} + (\Gamma_{fs} - \Gamma_{fc})e^{-(\dot{q}_{ai}/v_s)^2}]sign(\dot{q}_{ai}) \\ if \ |\dot{q}_{ai}| > 0 \ (slip) \\ min(|\Gamma_i - \Gamma_{ti}|, \Gamma_{fs})sign(\Gamma_i - \Gamma_{ti}) \\ if \ \dot{q}_{ai} = 0 \ (stick) \end{cases} \qquad (29)$$

where m_a is the actuator mass, k_t the stiffness of the joint, b_t the damping of the joint, Γ_{fs} the static friction force, Γ_{fc} the Coulomb friction force and v_s the sliding speed coefficient.

The linkage and effector dynamics are:

$$\Gamma_t = \hat{M}(P)\ddot{P} + \hat{N}(P,\dot{P}) \qquad (30)$$

$$\hat{M}(P) = \begin{pmatrix} m_{L1} + \frac{1}{2}(m - \lambda_1 + \lambda_2) & f_1(P) \\ m_{L2} + \frac{1}{2}(m - \lambda_2 + \lambda_1) & f_2(P) \end{pmatrix}$$

$$\hat{N}(P,\dot{P}) = \begin{bmatrix} r_{11} & r_{12} \\ r_{21} & r_{22} \end{bmatrix} \dot{P} + p(y)$$

$$\begin{cases} r_{11} = r_{21} \\ r_{12} = -[(2m_{L1} - 3\lambda_1 - \lambda_2)y^2 + (2m_{L1} - 3\lambda_1 - \lambda_2) \\ C(y)^2 + J_1 + J_2]\dot{y}/(2C(y)^3 \\ r_{22} = [(2m_{L2} - 3\lambda_2 - \lambda_1)y^2 + (2m_{L2} - 3\lambda_2 - \lambda_1) \\ C(y)^2 + J_1 + J_2]\dot{y}/(2C(y)^3 \end{cases}$$

where the mass linkage m_{Li} satisfies: $m_i = m_a + m_{Li}, i = 1, 2$.

Table 1: Parameters model of Biglide parallel robot.

Parameters	Values
Strut length (m) a	0.07
Mass (kg)	
m	0.034
$m1$	0.8040
$m2$	0.7940
First moment of links (kgm)	
ms_1	0.0045
ms_2	0.0043
Second moment of links (kgm^2)	
J_1	222.643×10^{-4}
J_2	2.539×10^{-4}
Gravity acceleration (ms^2)	
g	9.81
Additional parameter	
for the simulation model Mass (kg)	
λm	0.816